

# Supplementary Material

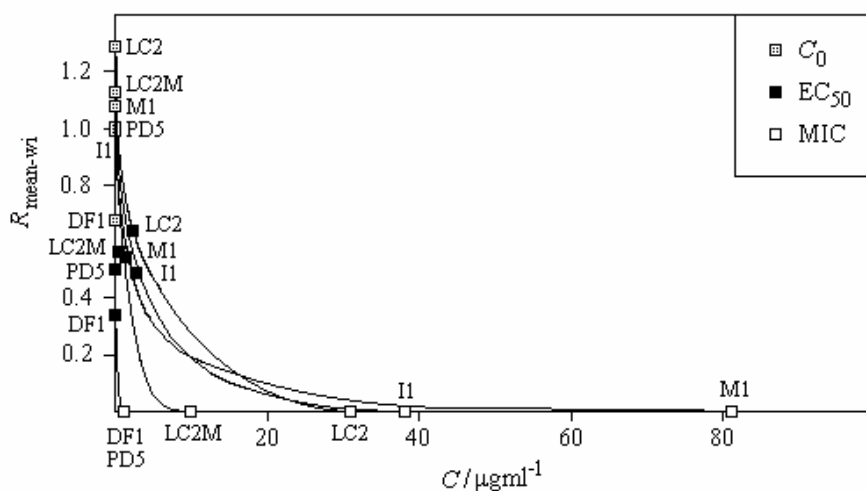
## Extensive chemometric investigations of the multidrug resistance in strains of the phytopathogenic fungus *Penicillium digitatum*

Rudolf Kiralj and Márcia M. C. Ferreira

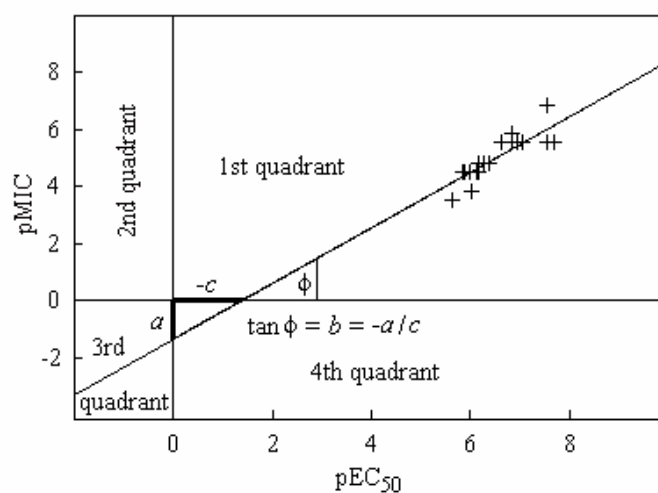
Laboratório de Quimiometria Teórica e Aplicada, Instituto de Química, Universidade Estadual de  
Campinas, Campinas, SP, 13083-970, Brazil

### CONTENTS

Figure F1. Relationship between biological activities $EC_{50}$ and MIC	II
Comments for Figure F1b	III
Table T1. Genome descriptors and experimental resistance activities (the data set C2)	IV
Figure F2. Minimum energy conformers for <b>I-VII</b>	V
Comments for Figure F2a	V
Comments for Figure F2b	VI
Figure F3. Superimposed <i>syn</i> - and <i>anti</i> - hydrogen bonding conformers	VII
Comments for Figure F3	VII
Figure F4. An experimental example of an <i>syn</i> -arranged azole in interaction with CYP51	VIII



a)



b)

**Figure F1.** Relationship between biological activities  $EC_{50}$  and MIC.

a) Reconstructed dose-response curves for triflumizole, showing the dependence of the mean growth radius ( $R_{\text{mean-wi}}$ , relative to strain PD5) on concentration  $C$  for six strains of different baseline DMI resistance.

b) Linear relationship  $pMIC = a + b pEC_{50}$  for experimental triflumizole data [20-24] with the geometrical definition of descriptors  $a$ ,  $b$ , and  $c$ . The values of the radius for zero-concentration ( $C_0$ ) were obtained from molecular graphics measurements of literature data [23], the mean values of all  $EC_{50}$  and some MICs were from literature [20-23], and MIC values for DMI-R strains were extrapolated from the linear relationship.

### Comments for Figure F1b

There are three types of pEC<sub>50</sub>-pMIC relationships, which can be visualized by different orientations and positions of the regression lines with respect to the four quadrants of the 2D Cartesian coordinate system.

1st type: The regression line for these toxicants does not pass the 2<sup>nd</sup> quadrant of the coordinative system, it is relatively close to the origin, and has a slope that approaches 45°.

2nd type: The regression line for these toxicants is relatively far from the origin, does not pass the 4<sup>th</sup> quadrant, and has a small slope.

3rd type: The regression line for these toxicants does not pass the 2<sup>nd</sup> quadrant, it is very far from the origin, and has a large slope.

These three types of behavior determine profiles of the dose-response curves for these toxicants with respect to each strain of *P. digitatum*.

Table T1. Genome descriptors<sup>a</sup> and experimental<sup>b</sup> resistance activities pEC<sub>50</sub> against DMIs (data set C2)

No.	Toxic./Strain <sup>c</sup>	PMR1-g	PMR1-e	CYP51-g	CYP51-e	PCR	PMR1-t	pEC <sub>50exp</sub>
93	C/PD5	1	1	1	1	0.25	100	6.604
94	C/DF1	1	1	1	1	0.25	100	6.847
95	C/U1	1	1	1	1	0.25	100	6.495
96	C/LC2	1	7	5	100	0.75	100	6.245
97	C/M1	1	7	5	100	0.75	100	6.002
98	C/I1	1	7	5	100	0.75	100	6.194
99	C/PD5	1	1	1	1	0.25	100	6.408
100	C/PD5-21	1	1	1	3	0.25	100	6.408
101	C/PD5-7	1	1	5	100	0.75	100	6.546
102	C/PD5-15	1	1	5	100	0.75	100	6.604
103	C/LC2	1	7	5	100	0.75	100	6.127
104	C/PD5	1	1	1	1	0.25	100	6.454
105	C/DISp12	0	0	1	1	0.25	1	6.428
106	C/DISp21	0	0	1	1	0.25	1	6.552
107	C/ECTp36	0	0	1	1	0.25	1	6.586
108	C/LC2	1	7	5	100	0.75	100	6.219
109	C/DIS33	0	0	5	100	0.75	1	6.449
110	N/PD5	1	1	1	1	0.25	100	5.723
111	N/DF1	1	1	1	1	0.25	100	5.626
112	N/U1	1	1	1	1	0.25	100	5.899
113	N/LC2	1	7	5	100	0.75	100	5.049
114	N/M1	1	7	5	100	0.75	100	5.026
115	N/I1	1	7	5	100	0.75	100	5.139
116	N/PD5	1	1	1	1	0.25	100	5.711
117	N/PD5-21	1	1	1	3	0.25	100	5.761
118	N/PD5-7	1	1	5	100	0.75	100	5.735
119	N/PD5-15	1	1	5	100	0.75	100	5.817
120	N/LC2	1	7	5	100	0.75	100	5.404
121	A/PD5	1	1	1	1	0.25	100	5.528
122	A/DF1	1	1	1	1	0.25	100	5.373
123	A/U1	1	1	1	1	0.25	100	5.771
124	A/LC2	1	7	5	100	0.75	100	5.216
125	A/M1	1	7	5	100	0.75	100	5.174
126	A/I1	1	7	5	100	0.75	100	5.350
127	A/PD5	1	1	1	1	0.25	100	5.651
128	A/PD5-21	1	1	1	3	0.25	100	5.636
129	A/PD5-7	1	1	5	100	0.75	100	5.699
130	A/PD5-15	1	1	5	100	0.75	100	5.528
131	A/LC2	1	7	5	100	0.75	100	4.967

<sup>a</sup>Six genome descriptors as reported in the literature [20-24], and estimated from these reports in cases of missing values.

<sup>b</sup>The pEC<sub>50exp</sub> activities from individual DMI sensitivity bioassays for 13 *P. digitatum* strains (wild types and mutants).

<sup>c</sup>Toxicants: C – cycloheximide (**V**), N – 4-nitroquinoline-*N*-oxide (**VI**) and A – acriflavine (**VII**).

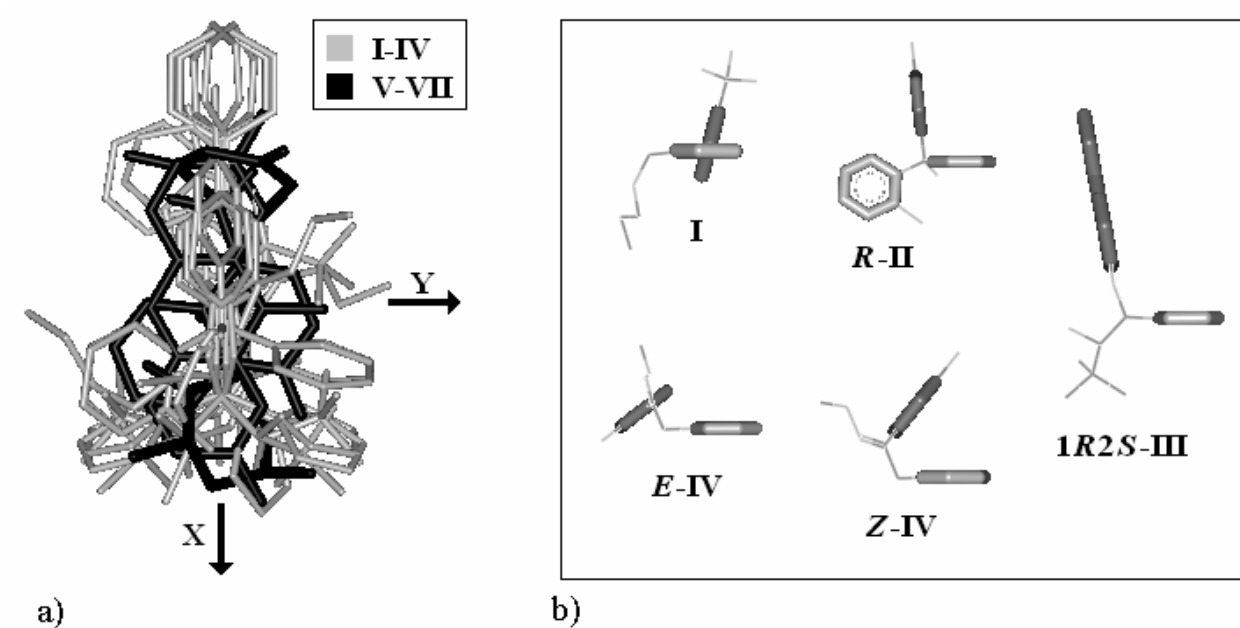


**Figure F2.** Minimum energy conformers for **I-VII**. a) Superimposed conformers for all isomers of **I-VIII** by their principal axes, with **I-IV** (DMIs) colored gray, and **V-VII** (non-DMIs) colored black. b) Selected minimum energy conformers of **I-IV** showing characteristic angles between the ring planes.

### Comments for Figure F2a

Structural features that distinguish DMIs and non-DMIs are visible in a). Flat **VI** and **VII**, and arc-like **V** (due to internal hydrogen bond and saturated rings) are not branched as DMIs. DMIs possess a central branching at tertiary or quaternary carbon and three side-chains of which two are necessarily ring structures. DMIs/non-DMIs difference in branching is best visible at the positive end of the inertial axis X.

**Comments for Figure F2b**

**IV**, the equimolar mixture of *E*- and *Z*-pyrifenoxy, according to ASRs, is a delocalized, conjugated and strained system that mimics a three-ring system. Such a structure is between other DMIs and planar mutagens **VI** and **VII**, because almost mutually perpendicular rings in isomers of **I-III** whilst the interplanar angles are smaller in *Z*- and *E*-**IV**.

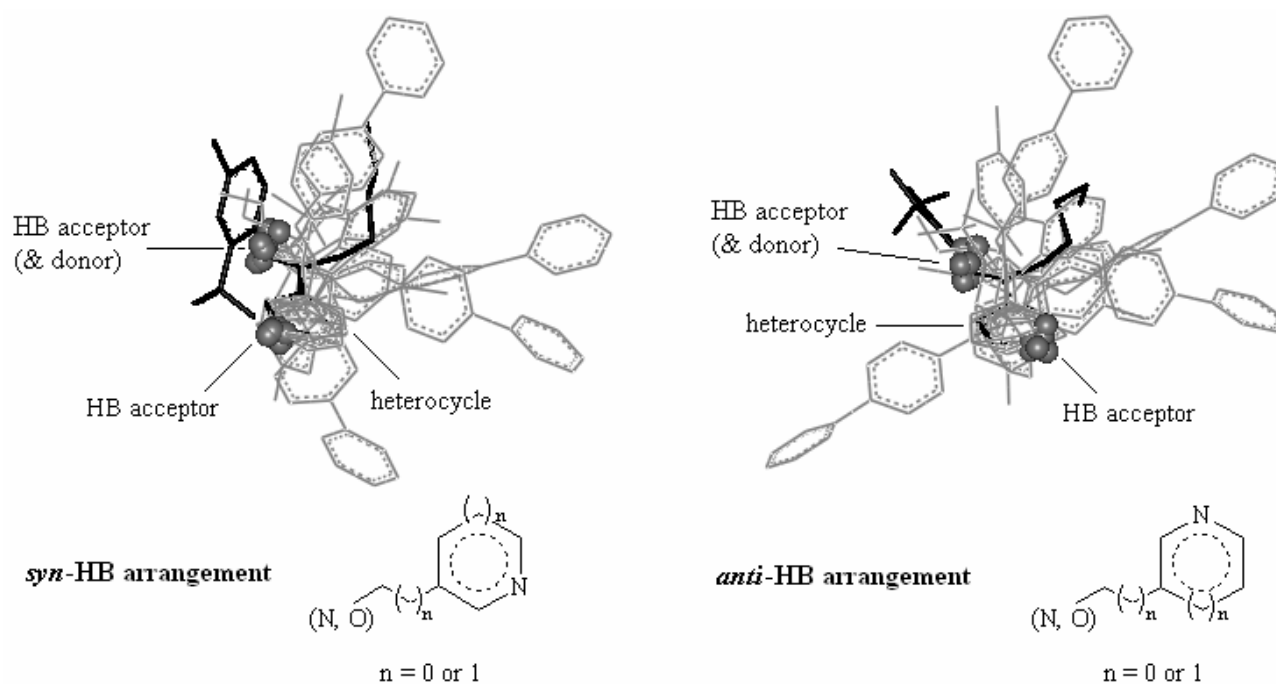


**Figure F3.** Superimposed *syn*- (a) and *anti*- (b) hydrogen bonding conformers of all isomers of **I-IV**, with corresponding two-dimensional topology. Triflumizole (**I**) is colored black, and the hydrogen bonding (HB) acceptors (and possible donors) are represented by balls.

### Comments for Figure F3

The HB *syn*-arrangements allow free access for one or even two HB groups of a receptor protein to the branching region, and another access for a HB donor to the heterocyclic exposed nitrogen (Fig. F3 left). The aromatic rings of all conformers are distributed in a wide range of directions behind and aside the HB region. However, the *anti*-arrangements enable only hydrogen bonds with the heterocyclic nitrogen, but the other HB acceptor's site is sterically hindered in most overlapped conformers, and the aromatic rings and chains are more dispersed than in the *syn*-conformers (Fig. F3 right). Hence, a transcriptional factor or an efflux pump component should possess a DMI binding site which would be highly hydrophobic and aromatic in one side, and with HB and polar groups in the other side. The heterocycle could bind between these two receptor's sides. But more conclusions cannot be made since there are no experimental structures of transcriptional factors in *P. digitatum* or other fungi, neither there are experimental structures of azole-efflux pump complexes.

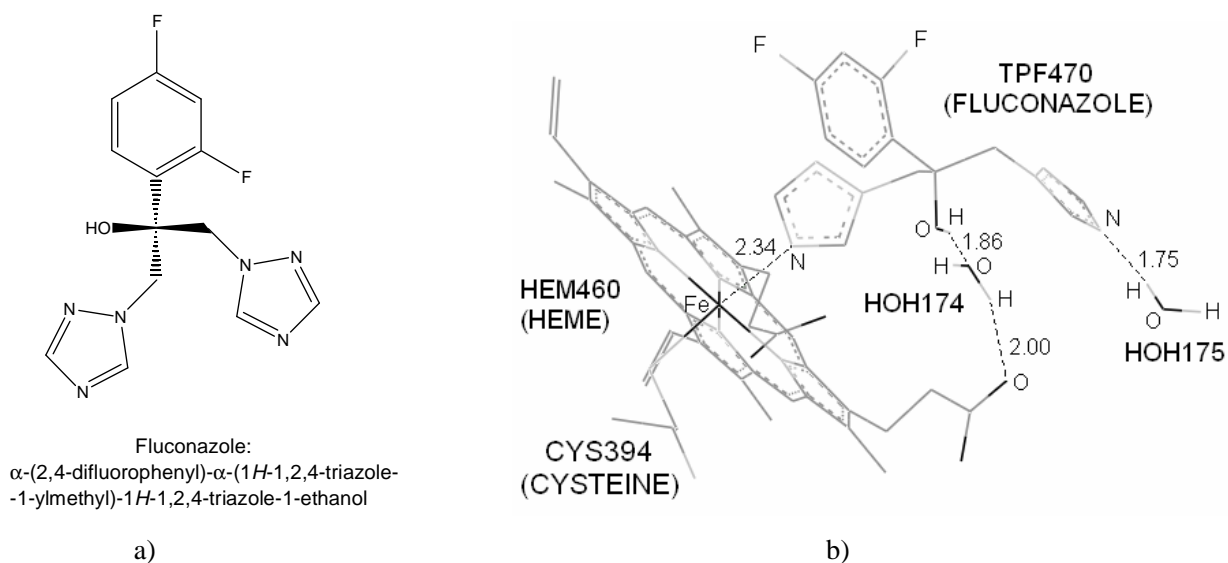


**Figure F4.** An experimental example of an azole in the *syn*-arrangement and its interaction with CYP51. a) Molecular structure of a DMI inhibitor fluconazole. b) Crystal structure of the active site of a CYP51-fluconazole complex (PDB: 1EA1 [7]), including the heme molecule chemically bonded to a cysteine and a triazole ring of fluconazole, two water molecules connected to fluconazole and heme *via* hydrogen bonds, and the fluconazole molecule. The *syn*-arrangement of N-Fe, O...H and N...H interactions is visible, with distances in Å units. The position of hydrogen atoms in water and the OH group was obtained at molecular mechanics MMFF94 level incorporated in the Titan program, with all other atoms frozen to preserve the original experimental geometry.